Elaboration of metallic compacts with high porosity for mechanical supports of SOFC

P.J. Panteix [a,*], V. Baco-Carles [a], Ph. Tailhades [a], M. Rieu [a], P. Lenormand [a], F. Ansart [a], M.L. Fontaine [b]

[a] Institut Carnot CIRIMAT (Centre Interuniversitaire de Recherche et d'Ingénierie des Matériaux), CNRS UMR 5085, Université Paul Sabatier, Bât II R1, 118 Route de Narbonne, 31062 Toulouse Cedex 4, France
[b] Institut Européen des Membranes, CNRS UMR 5635, Place Eugène Bataillon, 34095 Montpellier Cedex 5, France

A B S T R A C T

The development of third generation Solid Oxide Fuel Cells (SOFC) with metallic mechanical supports presents several advantages over that of ceramic stacks by offering a lower cost and longer lifetime of the stacks. As a consequence, it is necessary to prepare metallic porous compacts that remain stable at the operating temperature of the SOFC (700–800 °C) under reductive atmosphere. This paper presents an innovative process to elaborate iron, nickel and cobalt porous compacts. The process is based on the thermal decomposition of metal oxalate precursors with controlled morphology into metallic powders with coralline shape. Uniaxial compaction of such powders (without binder addition to the powders) under low uniaxial pressures (rising from 20 to 100 MPa) gave rise to green compacts with high porosity and good mechanical properties. After annealing at 800 °C under H_2 atmosphere, the compacts still present interconnected porosity high enough to allow sufficient gas flow to feed a SOFC single cell in hydrogen: the porosity rises from 25 to 50% for iron compacts, from 20 to 50% for cobalt compacts, and is higher than 40% for nickel compacts. Results from physicochemical characterization (XRD, SEM, gas permeation, Hg porosimetry) corroborated the process for SOFC application.

1. Introduction

The development of SOFC technology has been made in several steps, mainly driven by the aim to reduce the cost of the elementary cell. A planar configuration has been considered first with electrolyte mechanical support (1st generation – 1G SOFC): a high temperature (>1000 °C) is required to ensure sufficient ionic conductivity in the electrolyte (Yttria Stabilized Zirconia, most common electrolyte material) of great thickness (about several hundreds of micrometers). Due to this problem, the electrolyte thickness has then been reduced to 10–50 μm in the second generation (2G) of planar SOFC in order to allow a lower operating temperature (800 °C). Recently, it was proven that a third generation SOFC (Fig. 1) cell with a metallic mechanical support on which a thin layer of active material is deposited, would make possible to reach acceptable cost ranges. Indeed, the quantity of the ceramic materials, which is the cost-determining factor, has been reduced to the minimum. Resistance to mechanical breakdown induced by thermal cycles is improved by their good mechanical properties and the uniform distribution of temperature. The mechanical support is hence easier to weld or to connect [1–4].

Corresponding author. Tel.: +33 (0)5 61 55 61 20; fax: +33 (0)5 61 55 61 63.
E-mail address: panteix@chimie.ups-tlse.fr (P.J. Panteix).

Currently, one of the main challenges is to develop a metallic support with a controlled porosity, which means the possibility to adjust the pore size and porosity range. The issue is to maintain the substrates at sufficient porosity during co-firing and working of the cell for the feeding of fuel. On the other hand, the pores' size has to be adjusted in order to allow the deposition of the other elements of the single cell (e.g. the anode). This paper proposes a study of the feasibility of the adjustment of the porosity in iron, cobalt and nickel compacts. The final objective will be to prepare chemically stable alloys (such as Ni–Co, Fe–Ni–Co) under SOFC harsh working conditions. For instance, previous studies reported the development with commercial alloys and the evaluation of porous ferritic steels as CroFer22 APU for the same application [5,6]: the porosities were increasing from 30% [5] to 50% [5,6], with very large particles sizes (from 32 to 45 μm [5]) and large pores sizes (from 20 to 50 μm [6]).

The process proposed in our work offers two advantages: chromium free metal supports can be elaborated, and it is possible to adjust the proportion of porosity and the pore size. The process consists of two main steps: the elaboration of metal powders with a specific coralline morphology, followed by the uniaxial compaction of these powders. The metal powders elaboration is based on the thermal decomposition of precipitated oxalic precursors with well-controlled morphology in pure hydrogen [7–11]. It has been

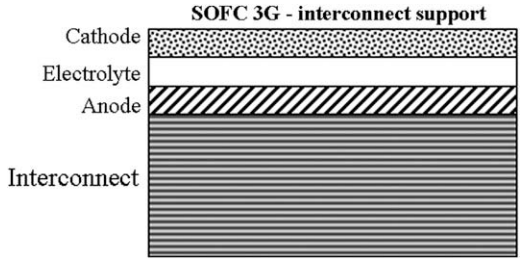

Fig. 1. Third generation SOFC planar cell configuration.

shown that an acicular shape of the oxalate particles induces, after reduction into metal, an entanglement of the elementary grains, giving rise to a coralline shape [8,9]. It is assumed that this specific morphology, characterized by a high shape irregularity, a strong surface roughness and also an important three-dimensional open porosity, results in a great overlapping of the adjacent filamentous grains during the compaction. Therefore, a rigid metallic skeleton was formed at low compaction pressures [10,11]. Other recent studies highlighted the importance of the metallic particles morphology and compaction pressure in reported results in the preparation of porous nickel membranes for the separation of ultrafine particles from gas [12–14]. Other methods such as the sinter/slurry (dispersion of the nickel grains in an organic binder) gave rise to porous nickel plaques for electrical backbones of electrode batteries [15], by using nickel powders with a branched chain or "filamentary" morphology obtained from nickel carbonyl decomposition [16].

The different steps of the process (from the preparation of the oxalate precursors to the sintering of the compacts at 800 °C in order to improve their mechanical strength) are presented here and results are discussed.

2. Experimental

2.1. Elaboration

2.1.1. Oxalate powders

Metallic salts $FeSO_4 \cdot 7H_2O$ (Prolabo, 99.5%), $NiCl_2 \cdot 6H_2O$ (Prolabo, 98.0%) and $CoCl_2 \cdot 6H_2O$ (Prolabo, 99.0%) were used for the synthesis of iron, nickel and cobalt oxalates precursors, respectively. The salt was dissolved in a hydro-alcoholic medium and slowly added to an acidified alcoholic solution of $H_2C_2O_4 \cdot 2H_2O$. The chemical parameters used for each synthesis are reported in Table 1. The precipitated oxalates were separated by filtration after 15 min and 1 h of aging for iron or cobalt and nickel, respectively. After washing with deionised water, and drying out at 80 °C, the three-oxalate powders were finally deagglomerated through a 250 μm sieve. The precipitation yields were around 80%.

2.1.2. Metallic powders and compacts

The nickel oxalate powder was reduced under dry hydrogen at 410 °C for 2 h, and the iron and cobalt oxalate powders were reduced under dry hydrogen at 520 °C for 2 h. During the thermal treatment, the oxalates $MeC_2O_4 \cdot 2H_2O$ were heated at 150 °C for 3 h before reaching the final temperatures (410 or 520 °C) to ensure complete dehydration of the powders (with a weight loss of about 20% corresponding to the departure of two constitution water molecules). The so obtained metal powders were deagglomerated through a 250 μm sieve.

Table 1
Chemical parameters used for the synthesis of metal oxalate powders.

Prepared powder	Metal salt	Oxalate salt	Addition flow ($L\,h^{-1}$)
$FeC_2O_4 \cdot 2H_2O$	$FeSO_4 \cdot 7H_2O$ ($1.0\ mol\,L^{-1}$)	$H_2C_2O_4 \cdot 2H_2O$ ($0.2\ mol\,L^{-1}$)	0.4
$NiC_2O_4 \cdot 2H_2O$	$NiCl_2 \cdot 6H_2O$ ($0.5\ mol\,L^{-1}$)	$H_2C_2O_4 \cdot 2H_2O$ ($0.2\ mol\,L^{-1}$)	1.2
$CoC_2O_4 \cdot 2H_2O$	$CoCl_2 \cdot 6H_2O$ ($1.0\ mol\,L^{-1}$)	$H_2C_2O_4 \cdot 2H_2O$ ($1.3\ mol\,L^{-1}$)	1.4

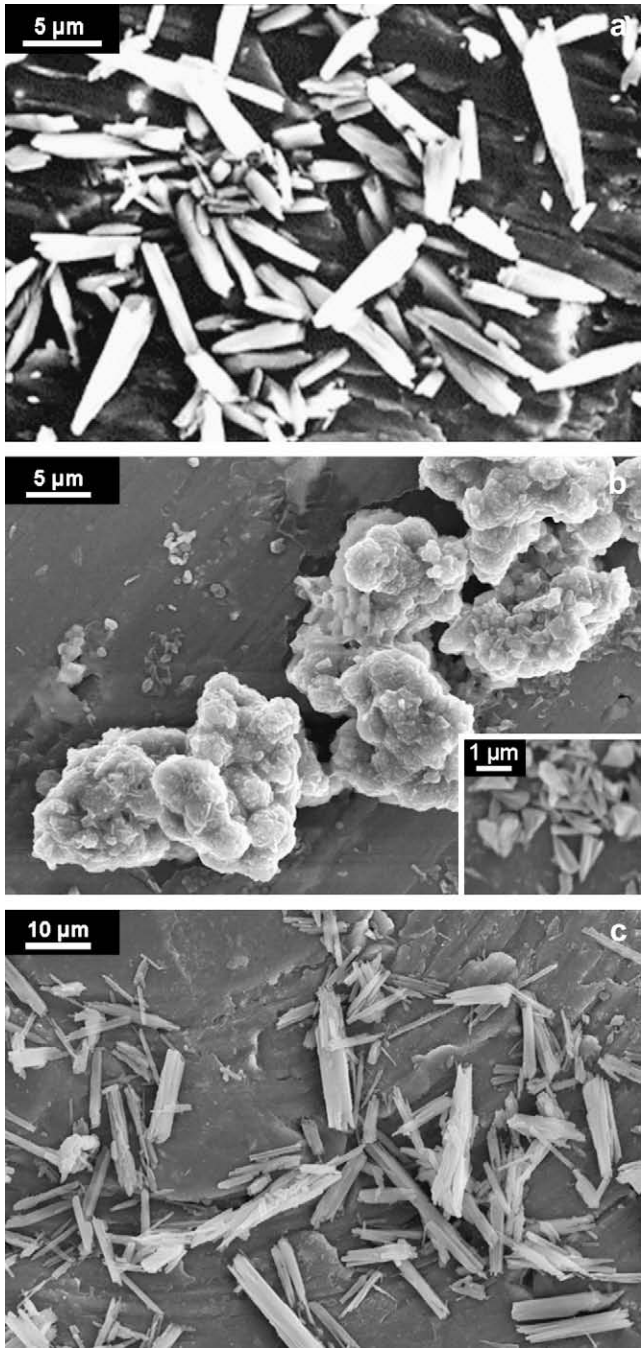

Fig. 2. Micrographs of the metal oxalate precursors: $FeC_2O_4 \cdot 2H_2O$ (a), $NiC_2O_4 \cdot 2H_2O$ (b) and $CoC_2O_4 \cdot 2H_2O$ oxalate (c).

The metallic powders were further compacted at 20 °C under uniaxial pressure without the addition of binder to the powders. The iron powder was compacted under 20, 30, 50 or 100 MPa, the nickel powder under 100 MPa and the cobalt powder under 30 or 100 MPa. Cylindrical pellets have been prepared: their green diameter was equal to 10 mm, and their green thickness was about 1 mm. Larger pellets were necessary in order to perform

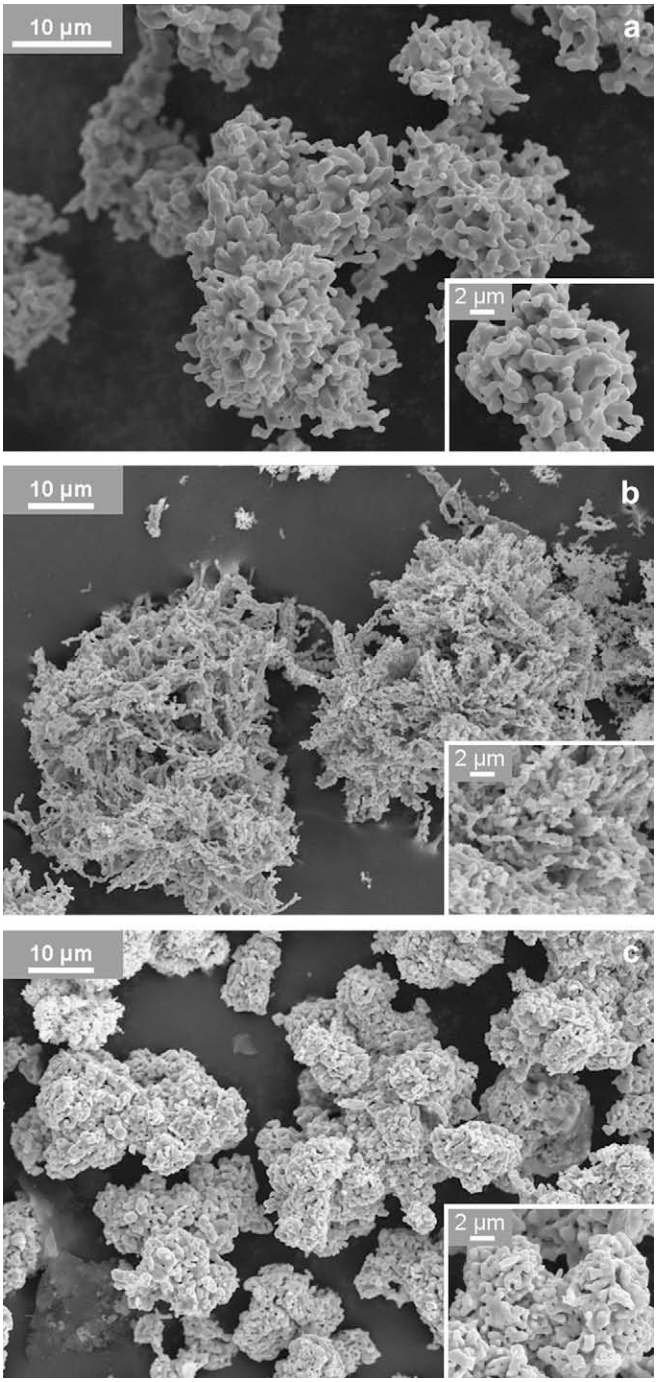

Fig. 3. Micrographs of the metallic powders after reduction under hydrogen: iron powder reduced at 520 °C (a), nickel powder reduced at 410 °C (b) and cobalt powder reduced at 520 °C (c).

permeance and Hg-porosimetry measurements: for these measurements, pellets with a green diameter and thickness of 20 mm and about 2 mm, respectively, were prepared for these characterizations. All the so made pellets have been sintered at 800 °C under hydrogen for 1 h.

2.2. Characterization

In order to determine the purity of the metal powders, thermogravimetric (TGA) analyses were carried out on a Setaram TG-DTA 92 microbalance with 20 mg of sample and alumina as reference.

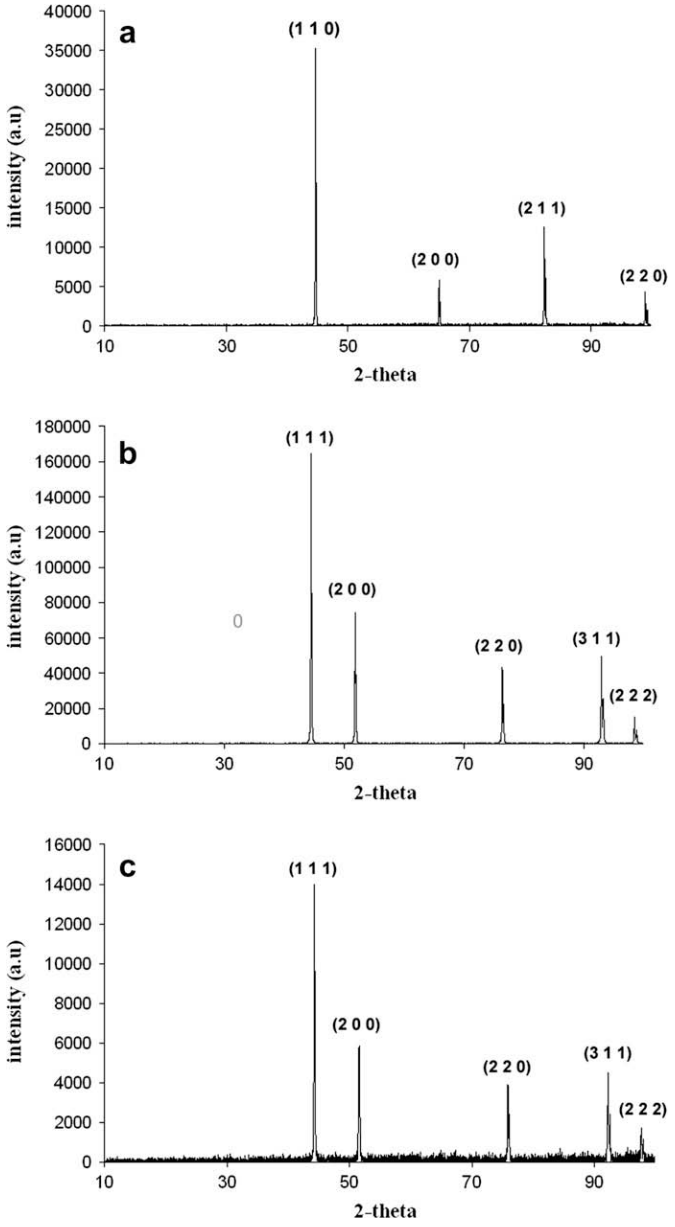

Fig. 4. X-ray diffraction patterns of iron powder reduced at 520 °C (a), nickel powder reduced at 410 °C (b) and cobalt powder reduced at 520 °C (c).

Phase detection of the oxalates and metal powders was carried out by XRD analysis with a Brucker D4 Endeavor diffractometer using a Cu Kα radiation source (Kα = 0.15418 nm).

Scanning electron microscopy (SEM) was used for morphological and microstructural investigation (JEOL JSM 6400, 20 kV accelerating voltage).

Table 2
Porosity of green metal compacts and of sintered metal compacts, and sintering behaviour of iron, nickel and cobalt pellets (green diameter = 10 mm) compacted under several uniaxial pressures.

Metal	P_c (MPa)	Green porosity (%)	Porosity after sintering (%)	Volume variations (%)
Fe	**20**	77	50	−53
	30	73	46	−51
	50	65	37	−47
	100	53	25	−39
Ni	**100**	56	44	−26
Co	**30**	81	49	−63
	100	60	20	−49

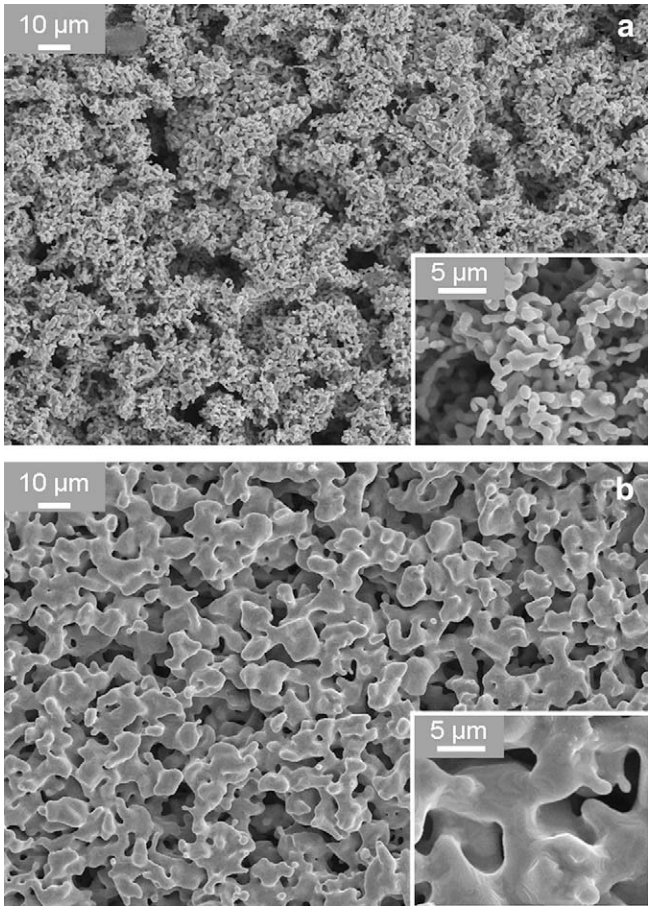

Fig. 5. Micrographs of the surface of a green iron pellet compacted under 20 MPa (a) and that of the same pellet after sintering at 800 °C under hydrogen (b).

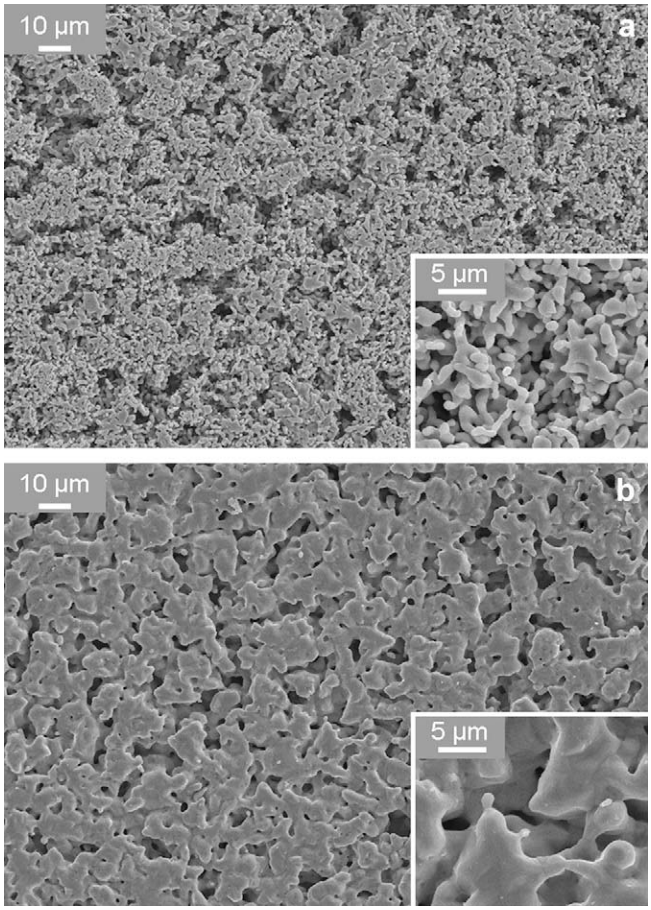

Fig. 6. Micrographs of the surface of a green iron pellet compacted under 100 MPa (a) and that of the same pellet after sintering at 800 °C under hydrogen (b).

The specific surface areas of the powders were measured by Brunnauer, Emmet and Teller (BET) method using N_2 adsorption at liquid N_2 temperature (1 point, analyzer Micromeritics DeSorb 2300A, USA).

The apparent density of the pellets was determined by geometrical measurements. The relative density of the pellets was obtained by considering the theoretical density values equal to 7.87 for iron metal, 8.91 for nickel metal and 8.90 for cobalt metal. The porosity values were deduced from the relative density values. Hg porosimetry (Micromeritics, Autopore IV 9500) has also been performed. The permeation of the pellets was measured with a permeation cell set up specifically designed for enabling membrane processing under high pressure (up to 10 bars) feed gas (N_2) at room temperature.

3. Results and discussion

3.1. Oxalate powders

X-ray diffraction patterns of the three oxalate powders revealed the diffraction peaks of the metastable form β of $MeC_2O_4{\cdot}2H_2O$ (Me = Fe, Ni or Co) [17–19].

The morphology of the oxalates powders (Fig. 2) is clearly acicular in the case of iron and cobalt oxalates (Fig. 2a and c). The iron oxalate powder $FeC_2O_4{\cdot}2H_2O$ (Fig. 2a) is homogeneous in size and shape: the average length and diameter of the particles are approximately 7 µm and 1 µm, respectively. The cobalt oxalate powder $CoC_2O_4{\cdot}2H_2O$ (Fig. 2c) is less homogeneous in size than iron oxalate. The particles tend to join together to form bundles, with length rising from 10 to 20 µm. The nickel oxalate powder $NiC_2O_4{\cdot}2H_2O$ (Fig. 2b) consists of very agglomerated submicronic needles.

3.2. Metal powders

The reduction temperatures have been optimized for each metal: the temperature must be high enough to allow the total decomposition of oxalates to metals, but not too high to prevent the sintering of the powders and to keep the intragranular porosity of the particles.

Micrographs of the reduced metals powders are presented on Fig. 3. In all cases, the entanglement of the original acicular oxalate particles during the thermal decomposition led to a coralline morphology of the corresponding metal particles. The partial sintering of the primary grains led to the formation of highly porous agglomerates (iron: 20–30 µm, Fig. 3a; nickel: 40–50 µm, Fig. 3b; cobalt: 10–20 µm, Fig. 3c). The specific surface area of the metal powders is equal to 0.5, 1.0 and 0.6 $m^2\,g^{-1}$ for the iron, nickel and cobalt powders, respectively.

X-ray diffraction patterns (Fig. 4) show that the oxalate precursor powders have been fully decomposed into metals. The iron powder (Fig. 4a) is alpha-type, with body centered cubic symmetry. Nickel and cobalt powders (Fig. 4b and c) are gamma-type with face centered cubic symmetry.

A little amount of the metal powders might be oxidized due to contact in air after the decomposition process under H_2 when the powders are removed from the thermal reactor. So the metal contents of iron and nickel powders have been determined by TGA

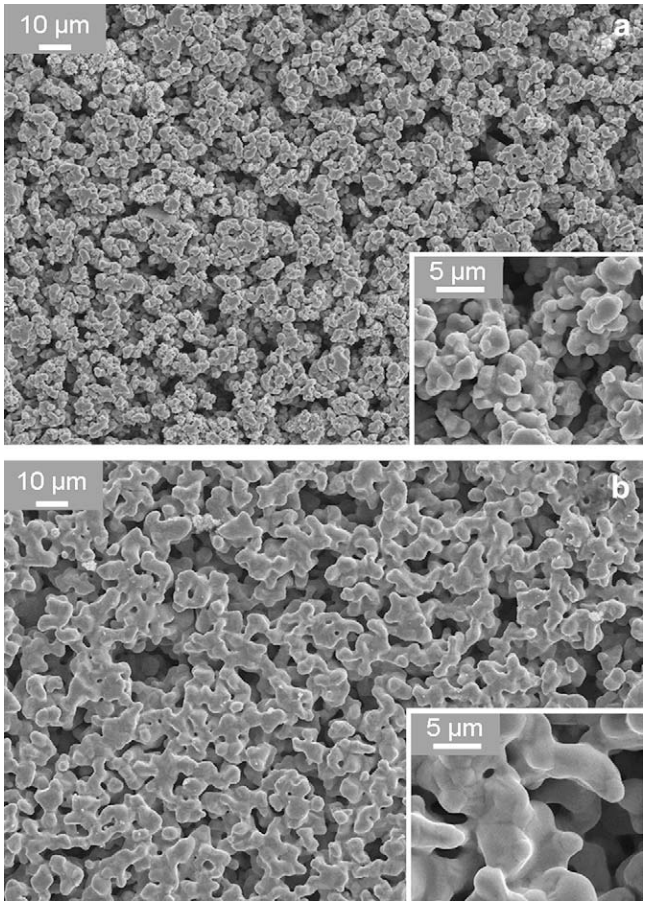

Fig. 7. Micrographs of the surface of a green nickel pellet compacted under 100 MPa (a) and that of the same pellet after sintering at 800 °C under hydrogen (b).

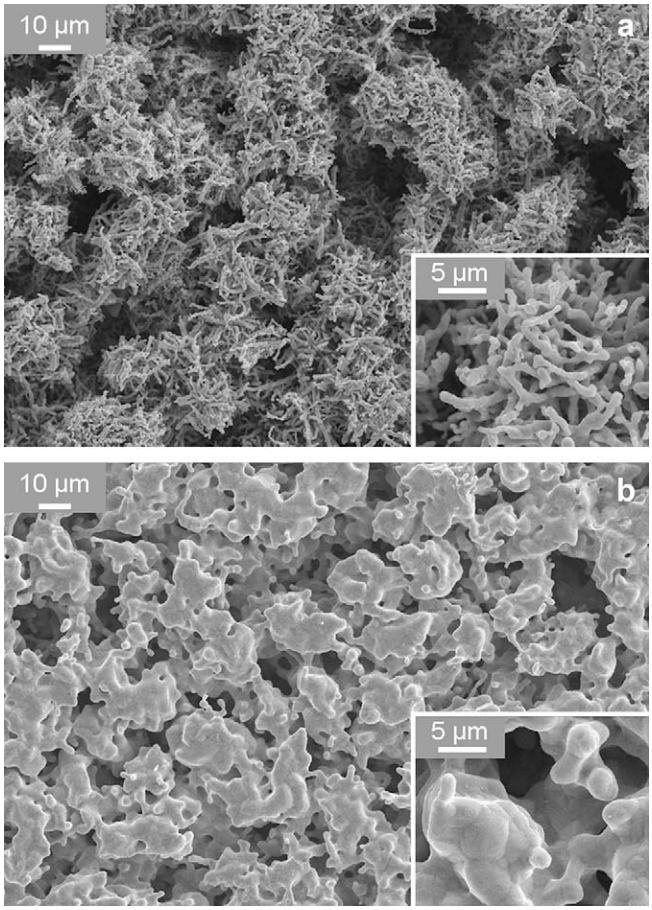

Fig. 8. Micrographs of the surface of a green cobalt pellet compacted under 30 MPa (a) and that of the same pellet after sintering at 800 °C under hydrogen (b).

analysis in air at 800 °C. The aim was to fully oxidize the iron and nickel powders into Fe_2O_3 and NiO, respectively, as follows:

$$(1 - x)Fe + xFe_3O_4 + (3/4 - 1/2x)O_2 \rightarrow (1/2 + x)Fe_2O_3$$

$$(1 - x)Ni + xNiO + (1/2 - 1/2x)O_2 \rightarrow NiO$$

Henceforth, the powders content of metal have been evaluated to 96.0 wt% and 98.0 wt% for the iron and nickel powders, respectively.

Contrary to the nickel and the iron powders, it is not possible to determine the cobalt purity by oxidation in air of the metal powder: indeed, the cobalt oxide CoO formed during the oxidation process gave a very compact protective layer surrounding the cobalt grains, avoiding the full oxidation of the metal core of the particles. Therefore it was necessary to perform TGA under H_2 to fully reduce the oxide to its metal:

$$(1 - x)Co + xCoO + xH_2 \rightarrow Co + xH_2O$$

The purity of the metal cobalt powder was thus evaluated to 99.0 wt%.

3.3. Metal compacts

Owing to the great compaction abilities of the metal powders, several uniaxial low compaction pressures have been performed in order to achieve coherent green compacts as porous as possible. The purpose of the heat treatment at 800 °C under H_2 was to increase the mechanical properties of the green pellets by initiating a partial sintering of the primary grains (creation of grain boundaries in keeping a porosity value high enough for the SOFC application). It was found that there is a correlation between the compaction pressure of the green pellets and the residual porosity measured after the heat treatment at 800 °C. Table 2 reports the porosity values and volume variations before and after the heat treatment. Figs. 5–9 present micrographs of the surfaces of iron, nickel and cobalt pellets compacted under several low compaction pressures (green and sintered pellets).

The compaction behaviour of the pellets depends on the morphology of the metal powders. The green strength of nickel pellets prepared with pressures lower than 100 MPa is too low to allow handling. This may be due to the morphology of the nickel powder, which is much less airy than the iron and cobalt ones (Fig. 3): consequently, the mechanical interlocking of adjacent primary grains is less favoured during the compaction. Hence only this compaction pressure has been studied for Ni. The iron and cobalt pellets have been prepared by using a large range of compaction pressures. It must be emphasized that both the iron pellet pressed under 20 MPa (77% porous, Fig. 5a) and the cobalt pellet pressed under 30 MPa (81% porous, Fig. 8a) present mechanical resistances high enough to allow handling. Furthermore, an iron pellet with diameter equal to 120 mm and thickness about 3 mm has been pressed under 30 MPa and presents a green porosity about 67%, showing the possibility to transpose the process to higher dimensions suitable for application in a complete SOFC single cell (Fig. 10).

According to the volume variations of the pellets during the heat treatment, the nature of the metal has a great influence on the

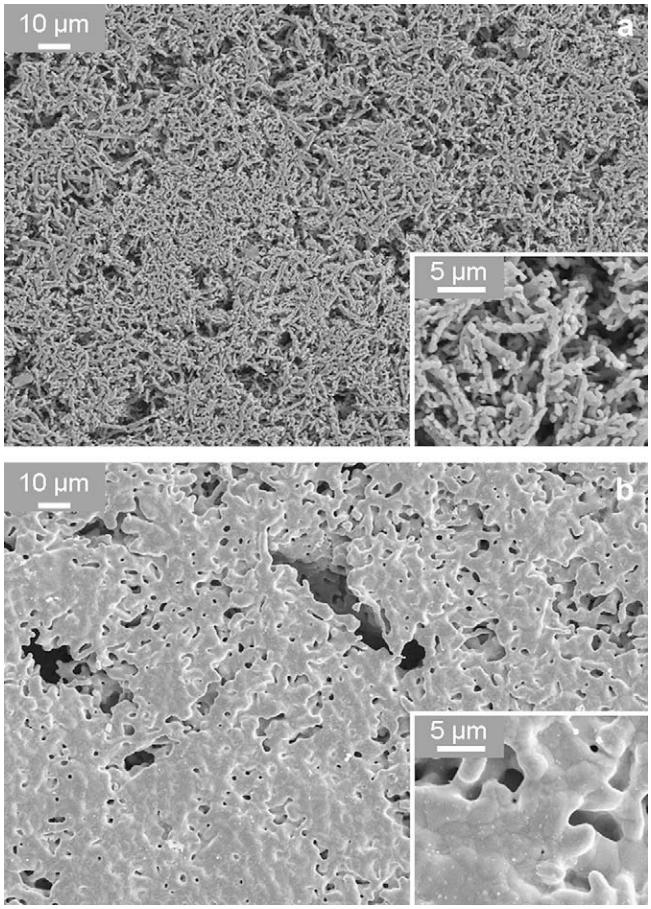

Fig. 9. Micrographs of the surface of a green cobalt pellet compacted under 100 MPa (a) and that of the same pellet after sintering at 800 °C under hydrogen (b).

sintering behaviour. As shown, the nickel pellet pressed under 100 MPa (Fig. 7a) has a green porosity equivalent to the green porosities of the iron (Fig. 6a) and cobalt (Fig. 9a) pellets prepared in the same conditions (56% vs. 53% and 60%, respectively). However, the shrinkage after heat treatment at 800 °C is much lower for the nickel pellets than that for the iron and cobalt ones. So the sintering ability of the nickel is lower than for the iron, which is

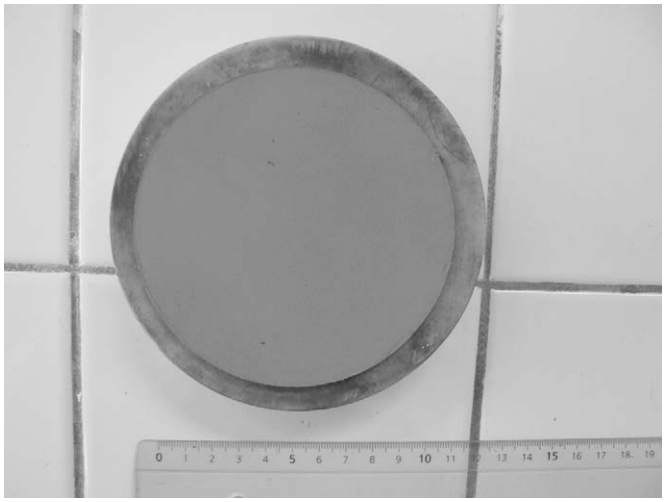

Fig. 10. Photograph of a green iron pellet pressed under 30 MPa, diameter = 120 mm; green porosity = 67%.

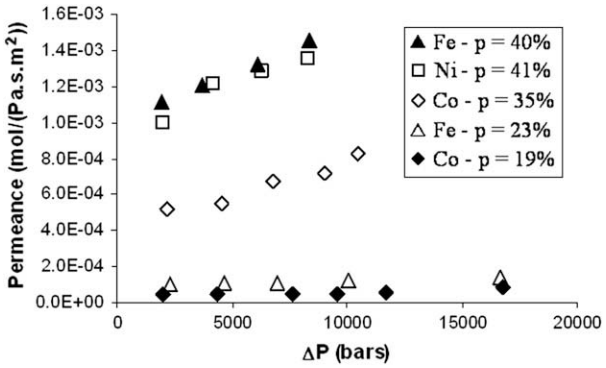

Fig. 11. Permeance behaviour of metal pellets with various porosities.

slightly lower than for the cobalt. This has been confirmed by the micrographs of the surface of the iron, nickel and cobalt pellets pressed under 100 MPa and sintered at 800 °C (Fig. 6b, Fig. 7b, Fig. 9b, respectively). In summary, iron and cobalt pellets with porosity varying on a large range (from 20 to 50%) can be prepared by controlling the uniaxial compaction pressure. The nickel pellets pressed under 100 MPa also exhibited a relatively high porosity after sintering (higher than 40%), which might be substantial for SOFC application.

Green pellets with green diameter equal to 20 mm were prepared in order to carry out further microstructural investigations as permeance and Hg-porosimetry measurements (Figs. 11 and 12 and Table 3). Iron pellets were compacted under 20 and 100 MPa, cobalt pellets under 30 and 100 MPa and a nickel pellet under 100 MPa. There is a good agreement between the values of porosity determined by geometrical measurements and the values of porosity measured by Hg porosimetry (Table 3). This indicates a complete open porosity of the pellets. Furthermore, the

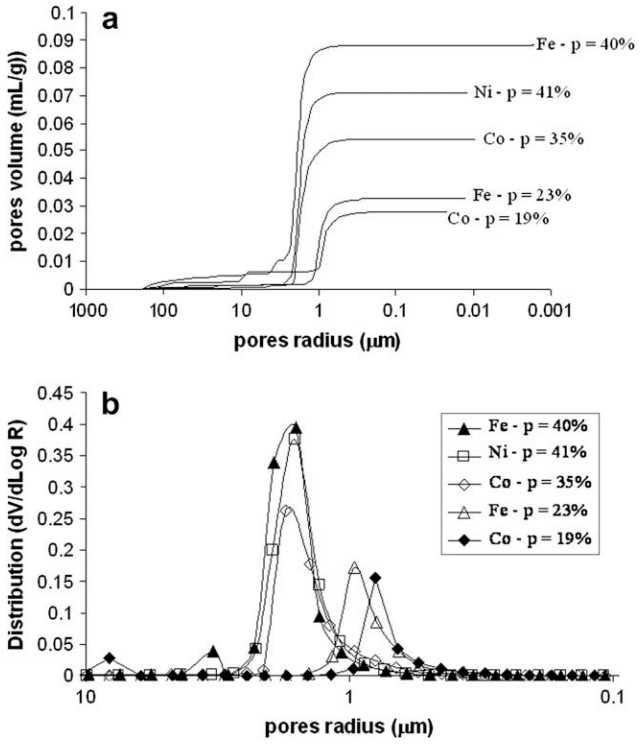

Fig. 12. Hg-porosimetry measurements carried out on metal pellets with various porosities: pores volume vs. pores radius (a) and pores distribution vs. pores radius (b).

Table 3
Results of Hg-porosimetry measurements on iron, nickel and cobalt pellets (green diameter = 20 mm) compacted under several uniaxial pressures.

Metal	P_c (MPa)	Geometrical green porosity (%)	Geometrical porosity after sintering (%)	Porosity after sintering measured by Hg porosimetry (%)	Mean pore size (μm)
Fe	**20**	73	40	40	1.9
	100	53	23	20	1.0
Ni	**100**	58	41	39	1.7
Co	**30**	76	35	33	1.7
	100	59	19	20	0.9

permeance results are coherent with the porosity values (Fig. 11): the more porous the pellets are, the higher is the gas flow across the pellet. The less porous pellets show very poor permeation behaviour, indicating that samples with porosity around 20% are worse candidates for SOFC applications.

The pore size measurements (Fig. 12, Table 3) show that the mean pore size and the pore volume decrease when the porosity of the pellets decreases. In every case, single dispersion of the pore sizes is observed (Fig. 12b). The mean pore size of the 35% porous cobalt pellet is very close to the pore sizes of the 40% porous iron pellet and of the 41% porous nickel pellet, but the permeation behaviour is worse (Fig. 11). The interconnected porosity of the cobalt pellet might be more tortuous than that of the iron and nickel pellets, resulting in less efficient gas flow across the pellet.

At this point, the metal compacts exhibit several of the characteristics required for an application as a metal support in a SOFC. A compromise could be found between the pores size and morphology to allow fuel supplying in avoiding the infiltration of anodic material efficiently. Furthermore, the resistance to corrosion in several atmospheres is another important point: the study performed here must be considered as a first approach to further work that will deal with the elaboration of metallic alloys presenting higher resistance to corrosion and the ability to adjust thermal expansion.

4. Conclusion

High purity iron, nickel and cobalt powders have been synthesized by thermal decomposition under H_2 from oxalate precursors. The acicular oxalate precursors led to metal grains with coralline morphology and high intragranular porosity. High porosity green pellets were prepared by uniaxial compaction. Further heat treatment at 800 °C under H_2 increased their mechanical strength and kept porosity values high. The compaction behaviours of the iron and cobalt pellets were very close: in both cases, a large range of green porosities was obtained by varying the compaction pressure (e.g. green porosity rising from 60 to 80% in the case of cobalt pellets), constantly yielding pellets which were easy to handle, whereas the nickel pellets had to be compacted under a minimum pressure of about 100 MPa to allow handling (green porosity equal to 56%). Furthermore, the iron and cobalt pellets presented similar sintering behaviours with high shrinkage, whereas the nickel pellets dimensions varied much less during the heat treatment at 800 °C under H_2. However, pellets with high porosity values have been obtained with the three metals studied here (porosities close to 50% for the most porous pellets of each metal).

The characterization of the permeance of the porous pellets showed that porosities higher than 35% are high enough to allow sufficient gas flow to feed a SOFC single cell in hydrogen. Contrary to the trends observed for the compaction and sintering behaviours, similarities have been observed for the porous structure (pore size, tortuosity) of iron and nickel pellets, with very efficient gas flow across 40% porous pellets, whereas the porosity of a 35% porous cobalt pellet appeared to be more tortuous, offering more indirect pathways for gas flow throughout the sample.

The process reported here has been used in order to prepare porous compacts with three single metals. It can be further applied to a wide variety of other metals or alloys (for instance Ni–Co, Fe–Ni–Co), thus rendering it as a very promising method to develop highly porous alloys for metallic interconnects in SOFC systems.

Acknowledgements

Authors would like to thank the A.N.R (Agence Nationale de la Recherche, 75012 Paris, France) for financial support of the CeraMet project.

References

[1] W.Z. Zhu, S.C. Deevi, Mater. Sci. Eng., A 348 (2003) 227.
[2] W.Z. Zhu, S.C. Deevi, Mater. Res. Bull. 38 (2003) 957.
[3] J.H. Zhu, S.J. Geng, D.A. Ballard, Int. J. Hydrogen Energy 32 (2007) 3682.
[4] J.W. Fergus, Mater. Sci. Eng., A 397 (2005) 271.
[5] R. Vaßen, D. Hathiramani, J. Mertens, V.A.C. Haanappel, I.C. Vinke, Surf. Coat. Technol. 202 (2007) 499.
[6] I. Antepara, I. Villarreal, L.M. Rodriguez-Martinez, N. Lecanda, U. Castro, A. Laresgoiti, J. Power Sources 151 (2005) 103.
[7] P. Tailhades, V. Carles, A. Rousset, FR Patent No. 9907340 (1999), EUR Patent No. 0401628.3-2309 (2000), US Patent No. 6, 464, 750 B1(2002).
[8] V. Baco-Carles, A. Arnal, D. Poquillon, P. Tailhades, Powder Technol. 185 (2008) 231.
[9] V. Baco-Carles, P. Combes, P. Tailhades, A. Rousset, Powder Metall. 45 (2002) 33.
[10] D. Poquillon, J. Lemaître, V. Baco-Carles, P. Tailhades, J. Lacaze, Powder Technol. 126 (2002) 65.
[11] D. Poquillon, V. Baco-Carles, P. Tailhades, E. Andrieu, Powder Technol. 126 (2002) 75.
[12] S.K. Ryi, J.S. Park, S.H. Choi, S.H. Cho, S.H. Kim, Sep. Purif. Technol. 47 (2006) 148.
[13] S.K. Ryi, J.S. Park, S.H. Kim, S.H. Cho, J.S. Park, D.W. Kim, J. Membr. Sci. 279 (2006) 439.
[14] S.K. Ryi, J.S. Park, D.G. Lee, S.H. Kim, J. Membr. Sci. 299 (2007) 174.
[15] E. Cormier, E.B. Wasmund, L.V. Renny, Q.M. Yang, D. Charles, J. Power Sources 171 (2007) 999.
[16] E.B. Wasmund, K.S. Coley, J. Mater. Sci. 41 (2006) 7103.
[17] H. Pezerat, J. Dubernat, J.P. Lagier, Compte-Rendu de l'Académie des Sciences Paris, France C266 (1968) p. 1357.
[18] R. Deyrieux, A. Peneloux, Bull. Soc. Chim. Fr. 8 (1969) 2675.
[19] P. Tailhades, Ph.D. Thesis, Toulouse, France, 1988.